



Climatic Factors Suppressing Tropical Cyclone Activity around Taiwan during October

Wei-Teh Li¹ · Jau-Ming Chen² · Ruo-Shan Tseng¹

Received: 31 January 2023 / Revised: 27 March 2023 / Accepted: 12 April 2023
© The Author(s) under exclusive licence to Korean Meteorological Society and Springer Nature B.V. 2023

Abstract

During Octobers of 1970–2019, no tropical cyclones (TCs) affected Taiwan in 32 out of 50 years (64%). Suppressed TC activity in these years results from different modulating processes imposed by various climatic features. During Octobers of El Niño years, TC genesis in the western North Pacific (WNP) shifts eastward and decreases in the western WNP to the southeast of Taiwan. An anomalous anticyclone across the South China Sea (SCS) and Taiwan hinders TC movement toward Taiwan. In La Niña years, TC genesis increases in the region southeast of Taiwan. These TCs are guided by an anomalous cyclone centering in the SCS to have major TC tracks to the southwest of Taiwan toward the SCS. A year with a September–November value on the Oceanic Niño Index (ONI) of between 0°–0.5 °C (–0.5°–0 °C) is categorized as a positive (negative) Normal year. During the positive Normal years, an anomalous cyclone over the WNP enhances TC genesis in its southern section and guides these TCs northward along the regions east of Taiwan. An anomalous anticyclone across the SCS and Taiwan hinders TC movement toward Taiwan. During the negative Normal years, a westward elongation of warm sea surface temperature anomalies from the WNP into the eastern Indian Ocean forces an anomalous anticyclone to extend westward from the WNP toward the SCS. TC genesis to the south of this anomalous anticyclone decreases and is accompanied by reduced TC movement toward Taiwan.

Keywords Tropical cyclone · Taiwan · October · ENSO

1 Introduction

In the western North Pacific (WNP), tropical cyclones (TCs) commonly cause devastation in countries within their propagation paths. The WNP TCs tend to follow three major tracks: westward toward southern China and the South China Sea (SCS), northwestward toward Taiwan and southeastern China, and northward toward South Korea and Japan (Camargo et al. 2007; Chu et al. 2010). Spatial patterns and strength of oceanic and atmospheric conditions are important factors affecting characteristics of TC genesis and their

propagation (e.g., Holliday and Thompson 1979; Chia and Ropelewski 2002; Kaplan and DeMaria 2003; Tippett et al. 2011). TCs tend to form within the monsoon trough (MT) assisted by favorable conditions such as strong vorticity, moist air, and enhanced convection (Gray 1968). After formation, steering flows guide TCs along different tracks (e.g., Harr and Elsberry 1991; Lander 1996). Steering flows are associated with variability in the Pacific subtropical high (PSH) and MT (Chen et al. 2009, 2019, 2020). From June to September, the western part of the PSH displaces northward reaching its northernmost position in August to September (e.g., Chen et al. 2017). TCs forming on its southern side within the MT tend to be steered northwestward by easterly/southeasterly flows, leading to Taiwan's peak TC season from July to September (Chen et al. 2007, 2010; Lai et al. 2022). The PSH starts to shift southward quickly in October and further southward to the south of 15°N in November and December (Chen et al. 2017). By October, TCs are guided westward across regions further to Taiwan's southern side, leading to reduced TC activity in Taiwan (Chen and Chen 2003). Statistics compiled by Taiwan's Central Weather

Responsible Editor: Pao-Shin Chu

✉ Jau-Ming Chen
cjming@nkust.edu.tw

¹ Department of Oceanography, National Sun Yat-Sen University, Kaohsiung, Taiwan

² Department of Maritime Information and Technology, National Kaohsiung University of Science and Technology, No. 482, Zhongjhou 3rd Rd., Kaohsiung 805, Taiwan

Bureau (CWB) for the period 1911 to 2021 (<https://www.cwb.gov.tw/V8/C/K/Encyclopedia/typhoon/index.html>) indicate that of the 371 TCs that affected Taiwan 26.1%, 29.1%, and 23.7% occurred during July, August, and September, respectively. This percentage dramatically reduces to just 8.1% in October, indicating a relatively low level of TC activity for this month.

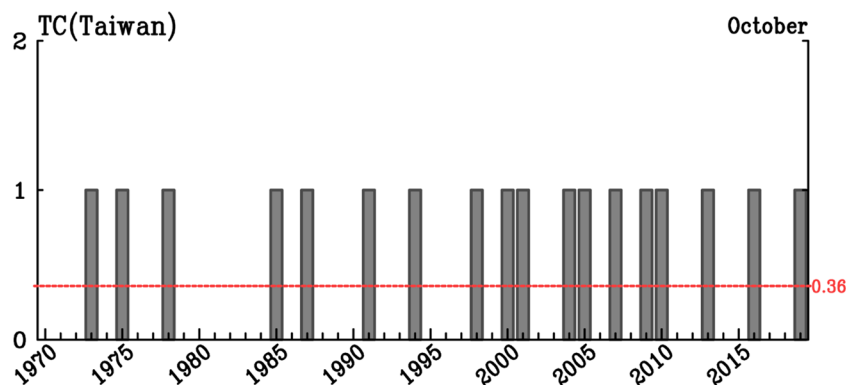
To further illustrate the notable weakening of TC activity during October, the 1970–2019 time series of TC numbers affecting Taiwan depicted by the Joint Typhoon Warning Center (JTWC) best track data is shown in Fig. 1. Taiwan is in a region 120°–122°E, 22°–25.5°N. In this study, TCs affecting Taiwan are defined as those moving through a region of 117°–125°E, 20°–28°N, which is within about 2–3 degrees of Taiwan. These TCs need to form in the WNP and reach an intensity of 34 kts or greater. During the past five decades, annually the number of TCs affecting Taiwan in October was either zero or one. There were 18 years with one TC, showing a long-term mean of 0.36. The other 32 years had no TCs affecting Taiwan making this phenomenon the dominant feature of Taiwan's October TC activity. This result led us to ask what major climatic factors suppress Taiwan's October TC activity.

Many aspects of TC activity in the WNP have been found to be evidently modulated by significant interannual variations of climatic states associated with El Niño Southern Oscillation (ENSO). Much previous research has shown that variations in TC genesis numbers and locations, TC intensity, and lifetime are affected by ENSO-related ocean-atmospheric anomalies (e.g., Chan 2000; Camargo and Sobel 2005; Chen et al. 2006; Li and Zhou 2013; Huang et al. 2017b; Chu and Murakami 2022). In general, ENSO-related tropical sea surface temperature (SST) anomalies effectively modulate atmospheric circulations that in turn cause changes in environmental factors such as relative vorticity, mid-tropospheric relative humidity, vertical motion, and vertical wind shear. TC genesis and movement are thus affected by these environmental changes (e.g., McPhaden 1999; Yeh et al. 2009; Wu et al. 2018; Chen et al. 2018b; Li et al. 2022). TC

movement from the WNP into the SCS during fall or into the northwestern North Pacific during summer was found to be enhanced or suppressed in either El Niño or La Niña events, revealing asymmetric ENSO-TC relationships for the WNP TC activity (Tan et al. 2019; Lai et al. 2021). Lai et al. (2022) showed that TC activity affecting Taiwan during the peak TC season (July–September) may be enhanced or suppressed during El Niño events but is generally suppressed during La Niña events. These results indicate that ENSO effectively influences TC activity around Taiwan. TC genesis in the WNP during the late season (October–December) exhibits a basin-wide interdecadal decrease around the late 1990s (Hsu et al. 2014; Shan and Yu 2020a). This is caused by a change toward La Niña-like climatic conditions over the past two decades, which have led to unfavorable dynamic conditions suppressing TC genesis over the WNP.

TC-induced rainfall during the TC season is an essential water resource for Taiwan (Chen et al. 2010, 2013a, 2018a, b; Chen and Chen 2011). It is, therefore, important to understand the modulating processes governing TC activity. Systematic ENSO modulations on TC activity in Taiwan during July–September have been delineated by Lai et al. (2022). However, how ENSO suppresses Taiwan's October TC activity resulting in zero TCs has not been comprehensively explored. Moreover, what are the differences in large-scale processes suppressing October TC activity between ENSO and non-ENSO (Normal) years? The main purpose of this study is to delineate large-scale processes suppressing TC activity in Taiwan during October. Differences in modulating processes between ENSO and non-ENSO years are compared to investigate the connections between different tropical SST anomalies and TC activity around Taiwan. Results of this study should advance our understanding of TC-climate interactions in hotspot zones of TC activity over the WNP and Taiwan. Moreover, comparisons in large-scale processes modulating TC activity between ENSO and non-ENSO years should give more insight into large-scale dynamic processes in the WNP.

Fig. 1 The 1970–2019 time series of TC numbers affecting Taiwan during October



2 Data

Four datasets are employed in various analyses in this study. Atmospheric anomalies are depicted by the National Oceanic and Atmospheric Administration (NOAA) monthly National Centers for Environmental Prediction-National Center for Atmospheric Research (NCEP-NCAR) reanalysis data (e.g., Kalnay et al. 1996). This dataset has a spatial resolution on a $2.5^\circ \times 2.5^\circ$ grid. Its winds at different levels and large-scale circulations (streamfunction and velocity potential) at 850 hPa are used to depict interannual variability of atmospheric circulations in the WNP. Variables of 850-hPa relative vorticity, 700-hPa relative humidity, 500-hPa vertical motion, and vertical wind shear between 200 and 850 hPa are used to examine effects of environmental factors on TC genesis. Oceanic anomalies are illustrated by the monthly extended reconstruction SST version 5 (ERSST-5) data (Huang et al. 2017a) with a $2^\circ \times 2^\circ$ global grid. Different SST variability imposes varying tropical forcing evoking atmospheric variability via air-sea interactions. ENSO and non-ENSO years are determined by the Oceanic Niño index (ONI). This index is represented by Niño 3.4 SST anomalies averaged over the tropical eastern Pacific ($120^\circ\text{--}170^\circ\text{W}$; $5^\circ\text{S}\text{--}5^\circ\text{N}$) (Xue et al. 2003). The ONI data are obtained from the Climate Prediction Center, NOAA. TC activity is portrayed by the 6-h best track dataset obtained from the Joint Typhoon Warning Center (JTWC). The JTWC dataset is used to delineate locations and numbers of TC genesis and TCs' movement tracks. Analyses in this study spans for a 50-year period from 1970 to 2019.

3 Different Climatic Types for October TC Activity in Taiwan

To delineate the major climatic factor associated with interannual variability in the tropical Pacific during October, the root-mean-square patterns of October SSTs during the period 1970–2019 are shown in Fig. 2. These patterns exhibit promising variability over the tropical eastern Pacific

around the Niño-3.4 region ($5^\circ\text{S}\text{--}5^\circ\text{N}$, $120^\circ\text{--}170^\circ\text{W}$), indicating ENSO as the dominant factor influencing interannual variability in the tropical Pacific during October.

For the period 1970–2019, there are 32 years (64%) with zero TCs affecting Taiwan and 18 years (36%) with one TC. These years are separated into two major groups associated with ENSO and non-ENSO states. In the ENSO group, El Niño and La Niña impose evidently different modulations on TC activity in the WNP via their opposite-polarity SST anomalies over the tropical eastern Pacific. It is legitimate to also separate the non-ENSO years into climatic types with positive and negative SST anomalies over the eastern tropical Pacific. Following the above separations, a year having an ONI value of 0.5°C and greater (-0.5°C and smaller) in both the September–November (SON) season and the ensuing winter (December–February) is defined as an El Niño (a La Niña) type. For the non-ENSO group, a year with an ONI value between $0^\circ\text{--}0.5^\circ\text{C}$ ($-0.5^\circ\text{--}0^\circ\text{C}$) in both SON and the following winter is sorted as a positive Normal (negative Normal) type. This classification of four climatic types allows us to compare the effects of ENSO and non-ENSO types as well as positive and negative tropical SST anomalies on TC activity over the WNP and Taiwan.

The member years and SON ONI values for the El Niño (EN), La Niña (LN), positive Normal (NM+), and negative Normal (NM-) types are illustrated in Table 1. For the zero-TC cases, there are 12, 10, 4, and 6 years in the EN, LN, NM+, and NM- types, respectively. For the one-TC cases, there are 5, 7, 1, and 5 years in the EN, LN, NM+, and NM- types, respectively. Differences in composite ONI means between zero-TC and one-TC cases are computed for different climatic types. Among them, the ONI difference is only significant in the LN type and insignificant in these other three types. For the LN type, composite ONI anomalies are colder in one-TC cases than zero-TC cases (-1.24°C vs. -0.91°C). However, ONI values range from -0.6°C to -1.5°C in zero-TC cases and from -0.6°C to -1.7°C in one-TC cases. It is difficult to differentiate zero-TC and one-TC cases based on only the ONI value in the LN years. The same is true for the other three climatic types.

Fig. 2 The root-mean-square patterns of tropical sea surface temperature (SST) during October from 1970 to 2019. Contour intervals are 0.1°C

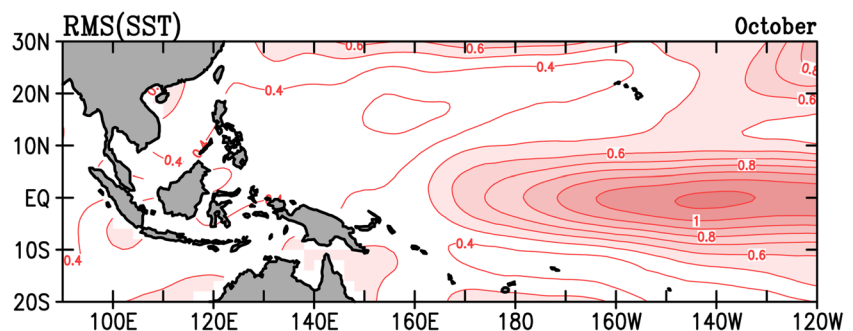


Table 1 The member years and Oceanic Niño Index (ONI) values in September–November (SON) for zero-TC and one-TC cases in Taiwan during October for difference climatic types. Differences of composite ONI means between zero-TC and one-TC cases significant at the 0.1 and 0.05 levels are marked by * and **, respectively

Climatic type	zero-TC cases		one-TC cases		Difference (one-TC– zero-TC)
	Year	ONI(SON)	Year	ONI(SON)	
El Niño (EN)	1972	1.8	1987	1.5	
	1976	0.8	1991	0.8	
	1977	0.7	1994	0.7	
	1979	0.5	2004	0.7	
	1982	2.0	2009	1.0	
	1986	0.9			
	1997	2.3			
	2002	1.2			
	2006	0.8			
	2014	0.5			
	2015	2.4			
	2018	0.8			
	mean: 1.23		mean: 0.94		-0.29
La Niña (LN)	1970	-0.7	1973	-1.7	
	1971	-0.9	1975	-1.4	
	1974	-0.6	1998	-1.4	
	1983	-0.8	2000	-0.6	
	1984	-0.6	2007	-1.3	
	1988	-1.5	2010	-1.6	
	1995	-1.0	2016	-0.7	
	1999	-1.3			
	2011	-1.0			
	2017	-0.7			
	mean: -0.91		mean: -1.24		-0.33**
positive Normal (NM+)	1990	0.3	2019	0.3	
	1993	0.1			
	2003	0.3			
	2012	0.3			
		mean: 0.25		mean: 0.3	
negative Normal (NM-)	1980	-0.0	1978	-0.3	
	1981	-0.1	1985	-0.3	
	1989	-0.2	2001	-0.3	
	1992	-0.2	2005	-0.3	
	1996	-0.4	2013	-0.2	
	2008	-0.4			
		mean: -0.22		mean: -0.28	

4 TC Variability Features and Modulating Processes in the ENSO Types

TC variability features associated with formation and movement are examined in terms of genesis frequency, passage frequency, and steering flows. Genesis frequency is depicted by TC numbers forming in every $5^{\circ}\times 5^{\circ}$ box during October. Passage frequency is estimated by counts of TC appearance in every $5^{\circ}\times 5^{\circ}$ box during October. Both the passage and genesis frequency are computed from the 6-h JTWC best track data. Genesis frequency portrays spatial patterns and density of TC formation, while passage frequency illustrates

major track patterns and density of TC movement. Steering flows (V_s) are vertically integrated from winds between 850 and 300 hPa reflecting influences of atmospheric flows on TC movement. Shan and Yu (2020b) pointed out that environmental steering flows exert dominant effects on guiding TC movement, while a deviation of TC movement from the steering flows is caused by beta drift.

In the ENSO types, there are 12 years in the EN type and 10 years in the LN type. Composite anomalies of passage frequency, genesis frequency, and steering flows for the EN type are shown in Fig. 3. Hereafter, composite anomalies reaching the 0.1 significance level of the Student-*t* test are

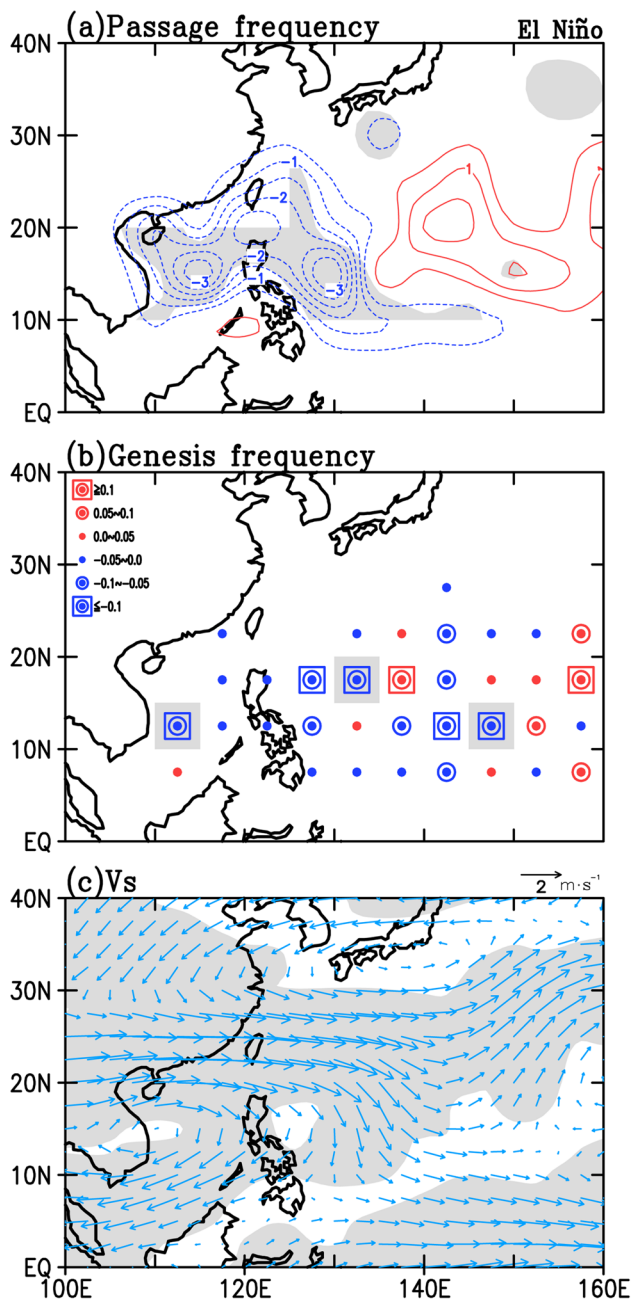


Fig. 3 Composite October anomalies of (a) TC passage frequency, (b) TC genesis frequency, and (c) steering flows integrated from 850 to 300 hPa for El Niño (EN) years with zero TCs affecting Taiwan. Contour intervals are 0.5 and the zero contours are suppressed in (a). Composite anomalies significant at the 0.1 level of the Student's t test are shaded

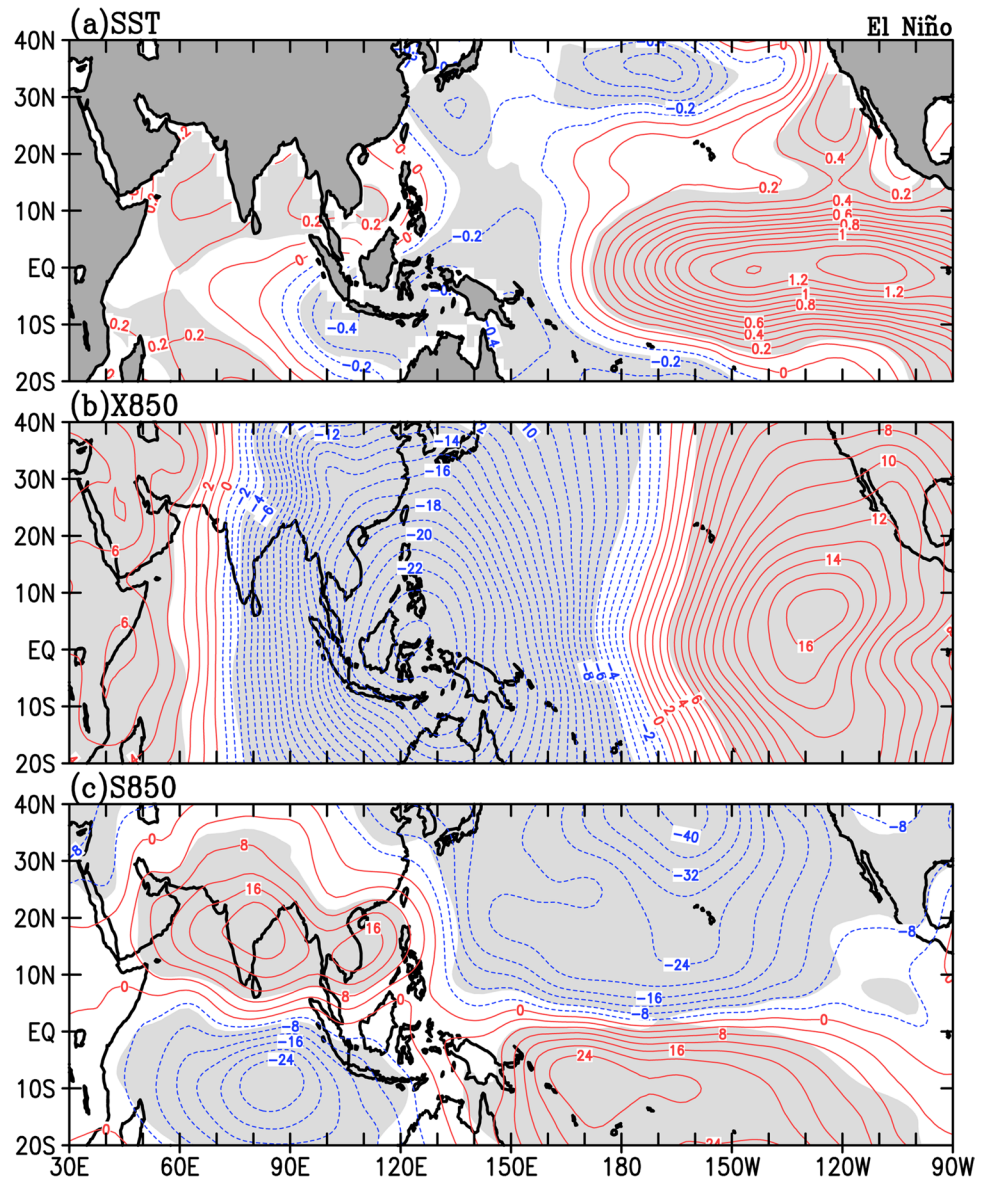
shaded. The Student- t test uses the formula of $t = \frac{\bar{x} - \mu_0}{s_x / \sqrt{n}}$, where \bar{x} is the mean of composite members, μ_0 is the mean of all members, $s_x = \sqrt{\frac{\sum_{i=1}^n (x_i - \bar{x})^2}{n-1}}$ is the standard deviation of composite members, and n is the number of composite

members. Composite anomalies of passage frequency (Fig. 3a) exhibit negative patterns in the SCS and in the WNP from the Philippine Sea northwestward toward Taiwan, corresponding to suppressed TC activity around Taiwan. Positive patterns exist in the regions east of 140°E. The above anomalous patterns of TC movement associate with a general increase (decrease) of TC genesis in the regions east (west) of 150°E (Fig. 3b). Composite anomalies of steering flows in Fig. 3c present a dominant anomalous anticyclone in the region west of 140°E with a center over the SCS and an anomalous cyclone to the north with a center around Japan. This anomalous cyclone extends southeastward to form cyclonic shears in the 140°–160°E, 10°–25°N region. These anomalous cyclonic shears set up favorable conditions for TCs forming in the region east of 150°E to move northwestward and result in positive anomalies in passage frequency. To the west of 150°E, anomalous westerly flows in the northern section of an anomalous anticyclone over 100°–140°E, 20°–30°N act to hinder the WNP TCs from moving northwestward toward Taiwan, leading to zero October TCs in Taiwan.

The large-scale modulating processes for TC activity are delineated by composite anomalies of SST and lower-tropospheric circulations in terms of 850-hPa velocity potential (X850) and 850-hPa streamfunction (S850). Composite SST anomalies (Fig. 4a) reveal a typical El Niño pattern. There are warm SST anomalies elongating in the tropical eastern Pacific and cold SST anomalies to the west in the WNP and tropical Indian Ocean divided by 165°E. Warm SST anomalies in the tropical eastern Pacific act as tropical heating to cause a large-scale convergent (positive) center in X850 anomalies (Fig. 4b). A large-scale divergent (negative) center appearing in the Maritime Continent around the 120°–130°E zone corresponds to tropical cooling associated with cold SST anomalies. Via a Matsuno-Gill-type response (Matsuno 1966; Gill 1980) to tropical forcing represented by anomalous X850 centers, S850 anomalies exhibit a meridional pair of anomalous cyclones (anticyclones) across the equator in the regions east (west) of the anomalous divergent center over the Maritime Continent (Fig. 4c). The significant anomalous anticyclone extending from the SCS eastward across Taiwan up to 130°E acts as the key feature suppressing TC activity in Taiwan. It is effective in blocking TCs' northwestward movement from the tropical WNP toward Taiwan via anomalous northwesterly flows (see Fig. 3b and c), yielding zero TCs in Taiwan during October in the EN type.

TC variability features for the LN type are illustrated in Fig. 5. Composite anomalies of passage frequency (Fig. 5a) exhibit a southwest-northeast contrast pattern. Increased TC movement appears from the Philippine Sea northwestward toward the SCS. On their northeastern side, decreased TC movement occurs along a northwestward

Fig. 4 Composite October anomalies of (a) SST, (b) 850-hPa velocity potential (X850), and (c) 850-hPa streamfunction (S850) for El Niño (EN) years with zero TCs affecting Taiwan. Contour intervals: (a) 0.1 °C, (b) $1 \times 10^5 \text{ m}^2 \text{ s}^{-1}$, and (c) $4 \times 10^5 \text{ m}^2 \text{ s}^{-1}$. Composite anomalies significant at 0.1 level of the Student's *t* test are shaded



path from the tropical WNP around the 140° – 160° E, 10° – 20° N region toward Taiwan. Composite anomalies of genesis frequency (Fig. 5b) reveal that TC genesis generally increases in the regions west of 150° E and decreases in the regions to the east. Steering flow anomalies (Fig. 5c) are noticed by an anomalous cyclone centering in the SCS and stretching southeastward across the Philippines toward the tropical WNP. On their northeastern side, an anomalous anticyclone has a center in the oceans between Taiwan and Japan and extends southeastward along the 20° – 35° N zone of the subtropical WNP. These circulation anomalies reflect TC genesis being suppressed by anticyclonic anomalies in the tropical region east of 150° E. Increased TCs forming in the tropical WNP west of 150° E are later guided by anomalous southeasterly flows in the northern section of the anomalous cyclone into the SCS, leading to

reduced TC movement toward Taiwan and zero October TCs.

Regarding large-scale modulating processes, composite SST anomalies (Fig. 6a) highlight a typical La Niña pattern featuring significant cold SST anomalies elongating along the tropical eastern Pacific and warm SST anomalies in the tropical WNP west of 160° E. In response to the east–west contrast of SST anomalies, composite X850 anomalies (Fig. 6b) exhibit a convergent center close to the Maritime Continent around the 120° – 135° E region and a divergent center in the tropical eastern Pacific around 120° W. These anomalous X850 centers largely coincide with the east–west distributions of underlying warm and cold SST anomalies across the tropical Pacific. The Matsuno-Gill-type response in composite S850 anomalies is clearly seen in Fig. 6c. With respect to the convergent center around the Maritime

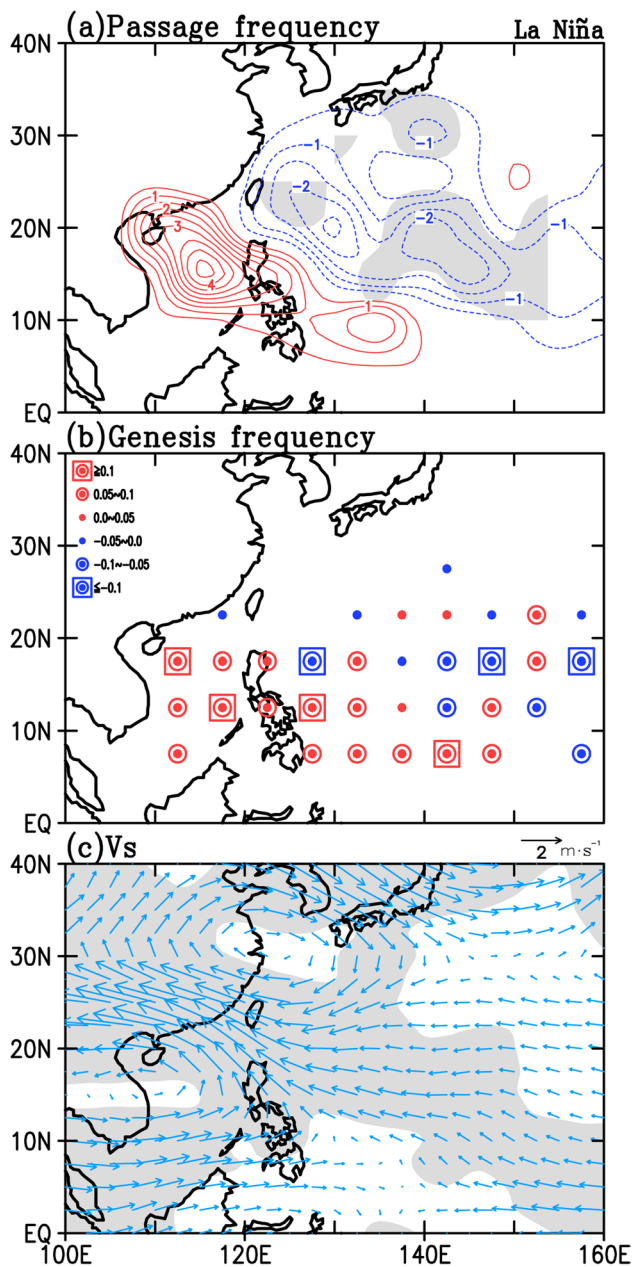


Fig. 5 Same as in Fig. 3, except for La Niña (LN) years

Continent, a pair of anomalous cyclones (anticyclones) appears on the two sides of the equator to the west (east) of 130°E . The anomalous anticyclone extending from the tropical WNP into the northwestern North Pacific acts to block the northward movement of the WNP TCs by which TCs tend to undergo a track in the tropical regions. Meanwhile, the significant anomalous cyclone over the SCS provides favorable conditions for TCs to move westward/northwestward from the tropical WNP into the SCS. As a result, TC activity is enhanced over the SCS but suppressed in the northern region over Taiwan (see Fig. 5a).

The above analyses demonstrate that TC genesis in the ENSO types exhibit a clear east–west contrast. TC genesis in the El Niño (La Niña) type tends to decrease (increase) in the tropical western WNP and increase (decrease) in the tropical eastern WNP divided by 150°E . Causes for the above genesis variability are investigated via environmental factors affecting TC genesis, including 850-hPa relative vorticity (ζ_{850}), 500-hPa vertical motion (ω_{500}), 700-hPa relative humidity (RH700), and vertical wind shear (VWS) of zonal wind between 200 and 850 hPa (Lai et al. 2021, 2022; Shan and Yu 2021; Tu et al. 2022). Composite anomalies of ζ_{850} , ω_{500} , RH700, and VWS for the El Niño and La Niña types are shown in Figs. 7 and 8, respectively.

In the El Niño type, decreased TC genesis in the tropical western WNP west of 150°E appears to be significantly affected by reductions in RH700 (Fig. 7c) and upward motion via positive ω_{500} anomalies (Fig. 7b). In the tropical WNP east of 150°E , increased TC genesis is facilitated by enhanced ζ_{850} (Fig. 7a) and weakened VWS (Fig. 7d). In the La Niña type, increased TC genesis in the WNP west of 150°E appears to be caused by enhancements in RH700 (Fig. 8c) and upward motion (Fig. 8b). In the region east of 150°E , decreased TC genesis appears to be suppressed by reduced ζ_{850} (Fig. 8a) and enhanced VWS (Fig. 8d). To quantitatively evaluate the significance of these modulating environmental anomalies, composite values of areal means of these environmental anomalies averaged over the tropical western ($120^{\circ}\text{--}150^{\circ}\text{E}$, $5^{\circ}\text{--}20^{\circ}\text{N}$) and eastern ($150^{\circ}\text{--}160^{\circ}\text{E}$, $5^{\circ}\text{--}20^{\circ}\text{N}$) WNP are shown in Table 2. The significant tests for these values reveal that in the El Niño (La Niña) type, decreased (increased) TC genesis in the tropical western WNP is significantly affected by ω_{500} and RH700 that corresponds with the suppressing (enhancing) effects of the overlying significant divergent (convergent) center in Fig. 4b (6b). In the eastern WNP, increased (decreased) TC genesis is significantly modulated by ζ_{850} and VWS associated with the favorable (unfavorable) effects imposed by a significant cyclonic (anticyclonic) circulation anomaly overlying this region as shown in Fig. 4c (6c).

In October, suppressed TC activity in Taiwan undergoes different modulating processes in the EN and LN types. In the EN type, the east–west contrast of SST anomalies in the tropical Pacific causes TC genesis to decrease in the western WNP. The anomalous anticyclone overlying the SCS and Taiwan further prevents TCs in the tropical WNP from moving northwestward toward the SCS and Taiwan, leading to suppressed TC activity in Taiwan. In the LN type, more TCs forming in the western WNP are mainly guided toward an anomalous cyclone centering in the SCS, leading to suppressed TC activity in the region north of the SCS over Taiwan.

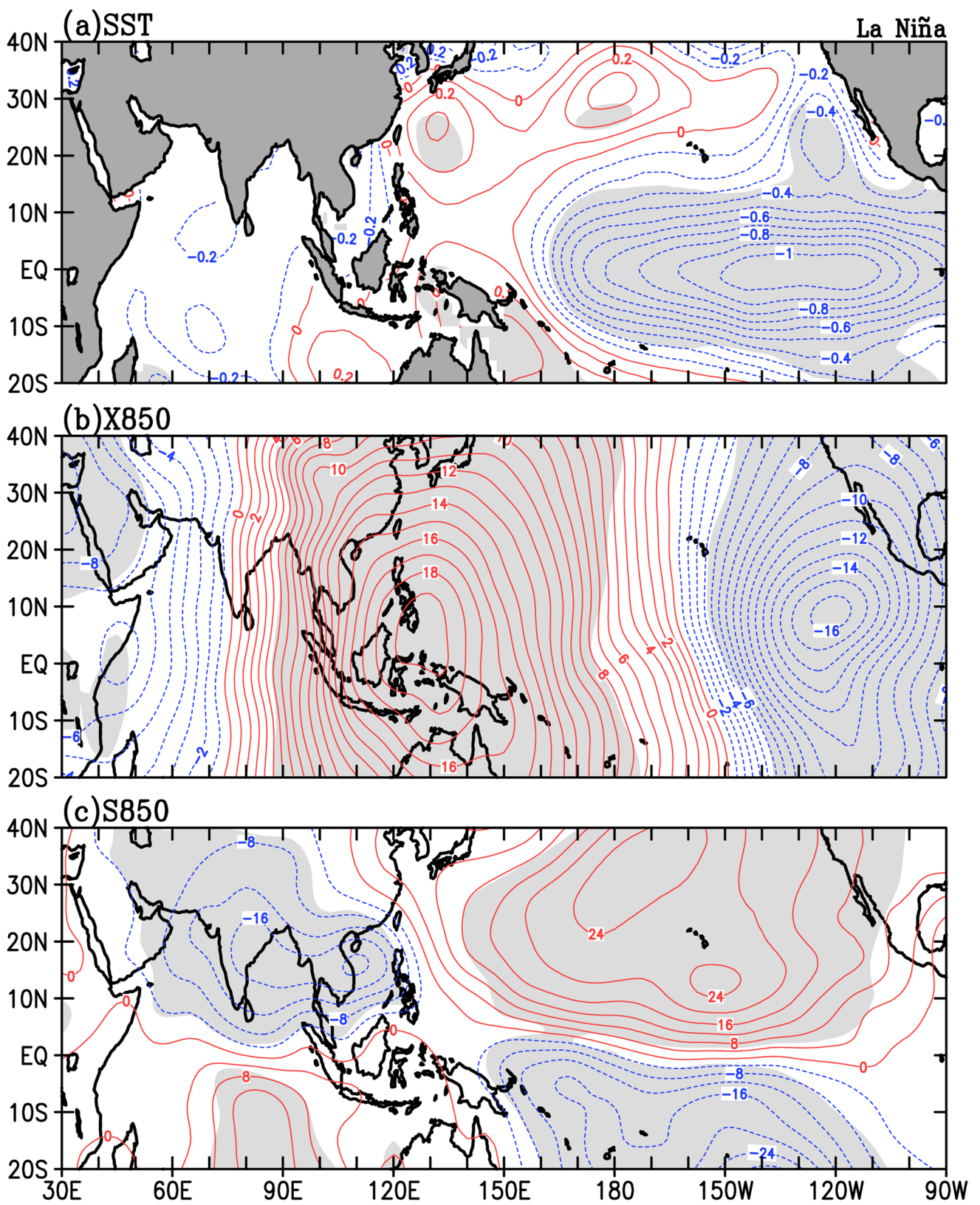
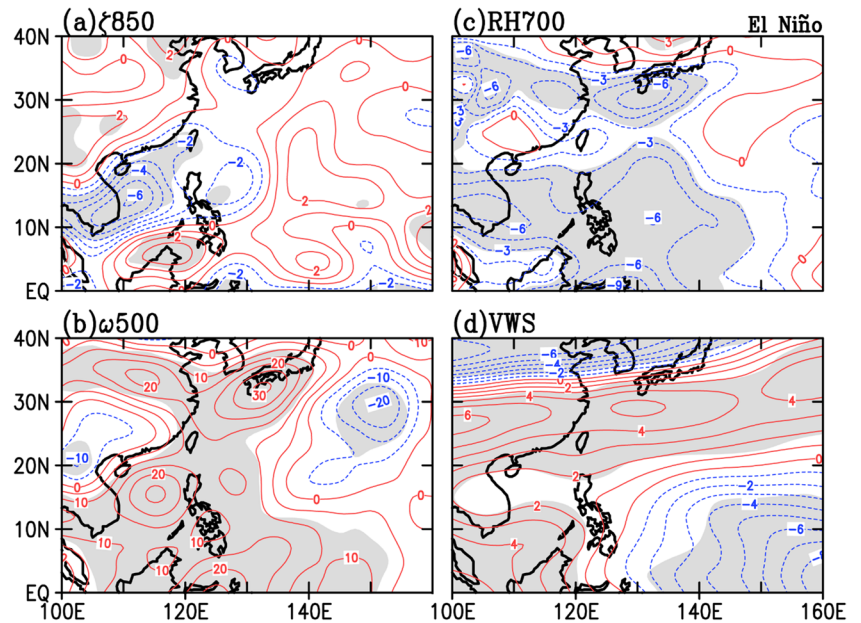


Fig. 6 Same as in Fig. 4, except for La Niña (LN) years

Fig. 7 Composite October anomalies of (a) 850-hPa relative vorticity (ζ_{850}), (b) 500-hPa vertical motion (ω_{500}), (c) 700-hPa relative humidity (RH700), and (d) vertical wind shear between 200-hPa and 850-hPa zonal winds (VWS) for El Niño (EN) years with zero TCs affecting Taiwan. Contour intervals: (a) $1 \times 10^{-6} \text{ s}^{-1}$, (b) $5 \times 10^{-3} \text{ Pa s}^{-1}$, (c) 1.5%, and (d) 1 m s^{-1} . Composite anomalies significant at 0.1 level of the Student-t test are shaded



5 TC Variability Features and Modulating Processes in the non-ENSO Types

For the non-ENSO types, there are four years in the positive Normal (NM+) type and six years in the negative Normal (NM-) type. During the Normal years without evident ENSO-related Pacific SST patterns, SST anomalies in the Indian Ocean (IO) and tropical North Atlantic (TNA) may exert evident influences on TC activity over the WNP. Wu et al. (2019) found that TNA SST anomalies evidently impact TC genesis over the northeastern WNP, but not

over the western WNP. Numerical experiments conducted by Yu et al. (2016) illustrated that TC activity over the WNP needs to be jointly modulated by SST anomalies from both the IO and TNA and is little affected by TNA SST anomalies alone. Zhan et al. (2011) demonstrated that warm (cold) SST anomalies in the eastern IO tend to suppress (enhance) TC genesis in the WNP. Such modulations are associated with changes in low-level relative vorticity and vertical motion (Wu et al. 2019). Ha et al. (2015) delineated that TC activity in the WNP is under the dominant influence of ENSO-related SST anomalies,

Fig. 8 Same as in Fig. 7, except for La Niña (LN) years

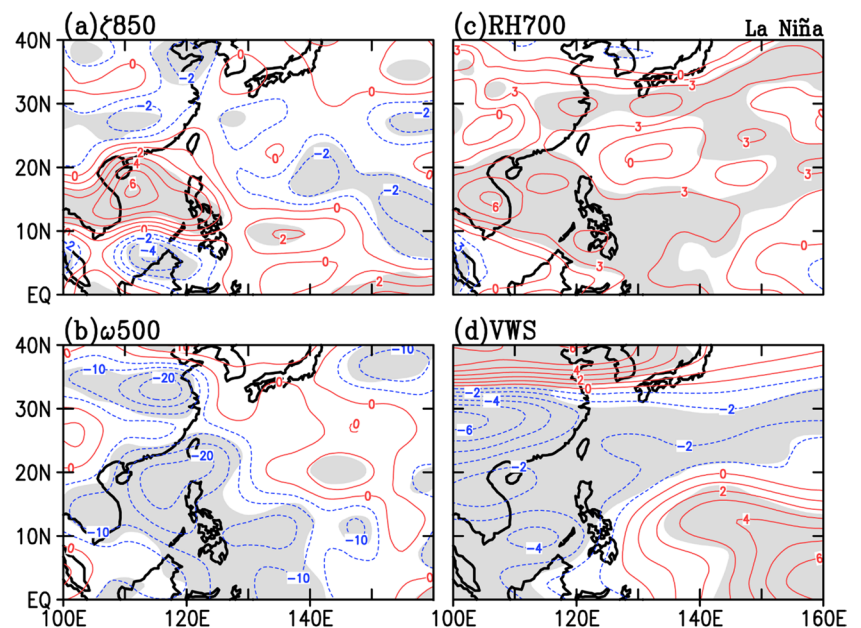


Table 2 Composite areal means of environmental factors affecting TC genesis in the ENSO types, including 850-hPa relative vorticity (ζ_{850}), 700-hPa relative humidity (RH700), 500-hPa vertical motion,and vertical wind shear of zonal wind between 200 and 850 hPa (VWS). Composite values significant at the 0.1, 0.05, and 0.01 levels of the Student-*t* test are marked by *, **, and ***, respectively

Climate type	Region	TC genesis	ζ_{850} (10^{-6} s^{-1})	ω_{500} ($10^{-3} \text{ Pa s}^{-1}$)	RH700 (%)	VWS (m s^{-1})
EN	120°-150°E	decreased	0.49	8.66***	-3.98***	-1.20
	5° -20°N					
	150°-160°E	increased	1.28**	2.43	-1.18	-4.25***
	5° -20°N					
LN	120° -150°E	increased	0.12	-8.73*	2.73**	0.66
	5° -20°N					
	150°-160°E	decreased	-1.21***	-2.25	1.07	2.96**
	5° -20°N					

while effects from eastern IO SST anomalies are secondary. These results indicate that IO SST anomalies may play a more important role than TNA SST anomalies in modulating TC activity over the western WNP and Taiwan. These modulating effects may become more noticeable during the Normal years.

For the NM+ type, composite anomalies of passage frequency (Fig. 9a) characterize two enhanced northward tracks. The first track is from the tropical WNP toward Japan in the 125°-135°E region. The second track moves northward in the 142°-147°E, 13°-21°N region and later turns northeastward. Composite anomalies of genesis frequency exhibit a meridionally stratified pattern. TC genesis tends to increase in the 15°-20°N zone of the WNP. To the south in the 5°-15°N zone, TC genesis increases in the region west of 130°E and decreases in the region to the east (Fig. 9b). Composite anomalies of steering flows exhibit a subtropical anomalous cyclone across the WNP with a center over Japan and an anomalous anticyclone centering in the SCS (Fig. 9c). The first and second enhanced northward tracks are associated with increased TC genesis in the southern sectors of the subtropical anomalous cyclone over the 125°-160°E, 15°-20°N zone. After formation, TCs along the first track are guided by the anomalous cyclone to move northward toward its central region to the northeast of Taiwan. On the other hand, an anomalous anticyclone over the SCS imposes anomalous northwesterly flows in its northern section to hinder TC movement from the tropical WNP toward the northern SCS and Taiwan, leading to suppressed TC activity in Taiwan. Decreased TC genesis in the regions to the south of 15°N and to the east of 130°E (Fig. 9b) corresponds to suppressed TC movement in that region (Fig. 9a).

For the NM+ type, composite SST anomalies exhibit major positive patterns in the tropical regions of the IO and central-eastern Pacific and negative patterns in the tropical western Pacific (Fig. 10a). These SST anomalies evoke large-scale convergent anomalies in the eastern Pacific and the western IO and a divergent anomaly between them

stretching meridionally from the Maritime Continent toward Taiwan and Japan in the 110°-140°E region (Fig. 10b). In response to these anomalous divergent centers, composite S850 anomalies exhibit a Matsuno-Gill-type pattern in the 70°-170°E, 20°S-40°N region (Fig. 10c), featuring a meridional pair of anomalous cyclonic (anticyclonic) circulations to the east (west) of the anomalous divergent centers around 125°E. The anomalous cyclonic circulation to the east of Taiwan acts to guide TCs forming in its southern section northward toward its central region south of Japan. In an opposite effect, the anomalous anticyclone across the northern SCS and Taiwan acts to prevent TCs from northwestward movement toward this region, leading to suppressed TC activity in Taiwan. These Matsuno-Gill-type circulation anomalies reveal that IO SST anomalies act to combine with the tropical Pacific SST anomalies to evoke anomalous divergent centers around the Maritime Continent and in turn affect large-scale circulation anomalies in the SCS and western WNP to suppress October TC activity over Taiwan during the NM+ type.

For the NM- type, major features in TC activity include enhanced northwestward and northward movement in the region east of 140°E (Fig. 11a) that is associated with increased TC genesis in the region east of 145°E (Fig. 11b). TC genesis in the 120°-145°E, 5°-25°N region tends to generally decrease, influenced by an anomalous anticyclone across this region (Fig. 11c). General increases in TC genesis and northward movement in the regions east of 145°E are assisted by an anomalous cyclone extending from Japan southeastward toward this region. There are two peculiar features in Fig. 11a including an extremely large positive anomaly of passage frequency at 130°E, 15°N and a minor positive anomaly northeast of Taiwan. Tracks of all October TCs included in the NM- type are displayed in Fig. 12 to delineate these two peculiar results. As denoted by a red line, typhoon Colleen in 1992 was formed at 0600UTC 18 October around 131.6°E, 11.8°N. It moved northward and looped around in the

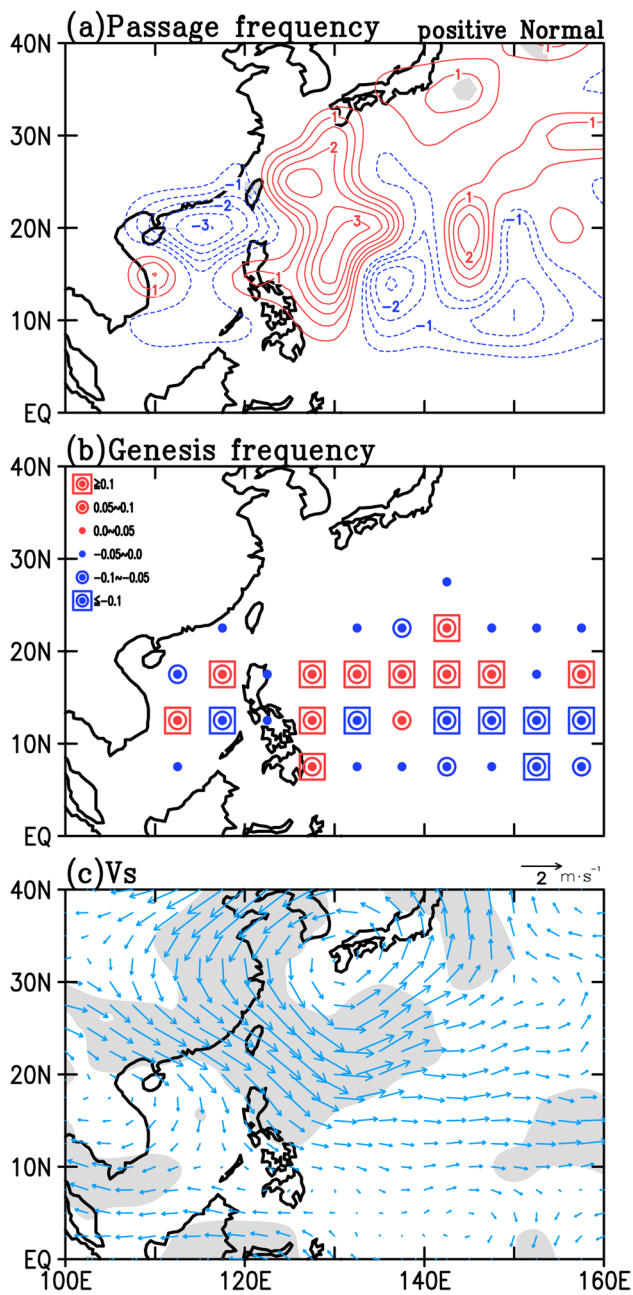


Fig. 9 Same as in Fig. 3, except for the positive Normal (NM+) years

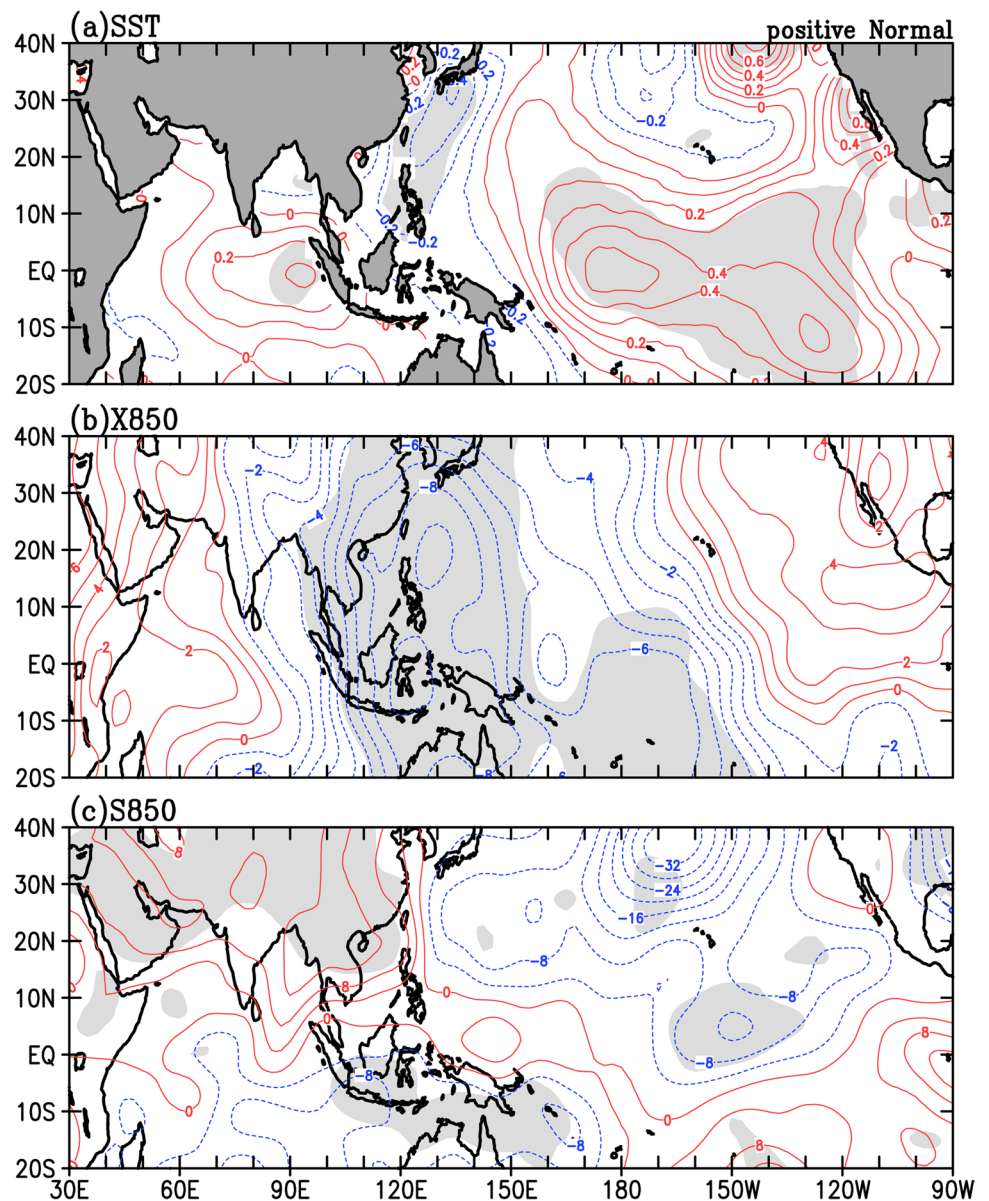
129.6°-130.9°E, 13°-14.4°N region for five days from 18 to 23 October before turning westward toward the SCS. This looping track causes a regional extreme value on a $5^\circ \times 5^\circ$ domain of passage frequency anomalies in Fig. 11a. In 1980, typhoon Wynne took a northwestward track and then recurved northeastward toward Japan with a turning point to the northeast of Taiwan. The slow movement around its turning path results in a minor positive anomaly to the northeast of Taiwan. Other than these two peculiar values, passage frequency anomalies to the east and southeast of

Taiwan over the 120°-140°E, 5°-25°N region exhibit a generally negative pattern.

For the NM- type, major tropical SST features are warm anomalies across the eastern IO, the Maritime Continent, and the tropical western Pacific (Fig. 13a). In response to these warm SST anomalies, composite X850 anomalies exhibit a significant convergent center around the Maritime Continent (Fig. 13b). It further excites S850 anomalies to reveal a Matsuno-Gill-type pattern in the 60°-160°E, 20°S-40°N region (Fig. 13c), characterized by a meridional pair of anomalous anticyclonic (cyclonic) circulations to the east (west) of the tropical convergent center around 110°E. Among these circulations, an anomalous anticyclone stretches from the WNP westward across Taiwan toward the SCS and acts to reduce TC genesis in its southern section over the tropical WNP. Consequent TC movement toward the north is hindered resulting in no TCs in Taiwan during October. These results reveal that warm SST anomalies in the tropical eastern IO and the Maritime Continent act as the center of action evoking large-scale circulation anomalies across the IO and WNP by which TC activity in Taiwan is suppressed in the NM- type.

Variability in TC genesis in the non-ENSO types does not exhibit systematic spatial features typical of the ENSO types. TC genesis in the NM+ type has a meridional contrast over the WNP with a northern increase and a southern decrease divided by 15°N. There is a general decrease in TC genesis in the western WNP for the NM- type. Composite anomalies of environmental factors for the NM+ and NM- types are shown in Figs. 14 and 15, respectively. In the NM+ type, decreased TC genesis in the WNP south of 15°N relates to reduced ζ_{850} (Fig. 14a) and upward motion (Fig. 14b). Increased TC genesis in the 15°-20°N zone connects with enhanced ζ_{850} and RH700 (Fig. 14c) and weakened VWS (Fig. 14d). For the NM- type, decreased TC genesis in the western WNP (120°-145°E, 5°-25°N) corresponds with mixed positive and negative anomalies of all environmental factors (Fig. 15). To quantitatively measure the gross impact of environmental factors on TC genesis, composite areal means of these factors averaged over the southern WNP (130°-160°E, 5°-15°N) and northern WNP (125°-160°E, 15°-20°N) for the NM+ type and over the western WNP (120°-145°E, 5°-25°N) for the NM- type are displayed in Table 3. In the NM+ type, decreased TC genesis over the southern WNP is hindered by insignificant anomalies of reduced ζ_{850} and upward motion. Increased TC genesis in the northern WNP is facilitated by all four environmental factors with significant effects from ζ_{850} and RH700. In the NM- type, decreased TC genesis in the western WNP is associated with insignificant anomalies of reduced ζ_{850} and strengthened VWS. Since climatic anomalies in the non-ENSO types are much weaker than those in the ENSO types, environmental factors in the non-ENSO types thus exert less

Fig. 10 Same as in Fig. 4, except for the positive Normal (NM+) years



significant and systematic impact on TC genesis in the WNP than that by the ENSO types. Among them, ζ_{850} acts as the only factor to positively modulate variability of TC genesis in the WNP for both the NM+ and NM- types, reflecting the major modulating effects from overlying circulation anomalies on TC genesis in the non-ENSO types.

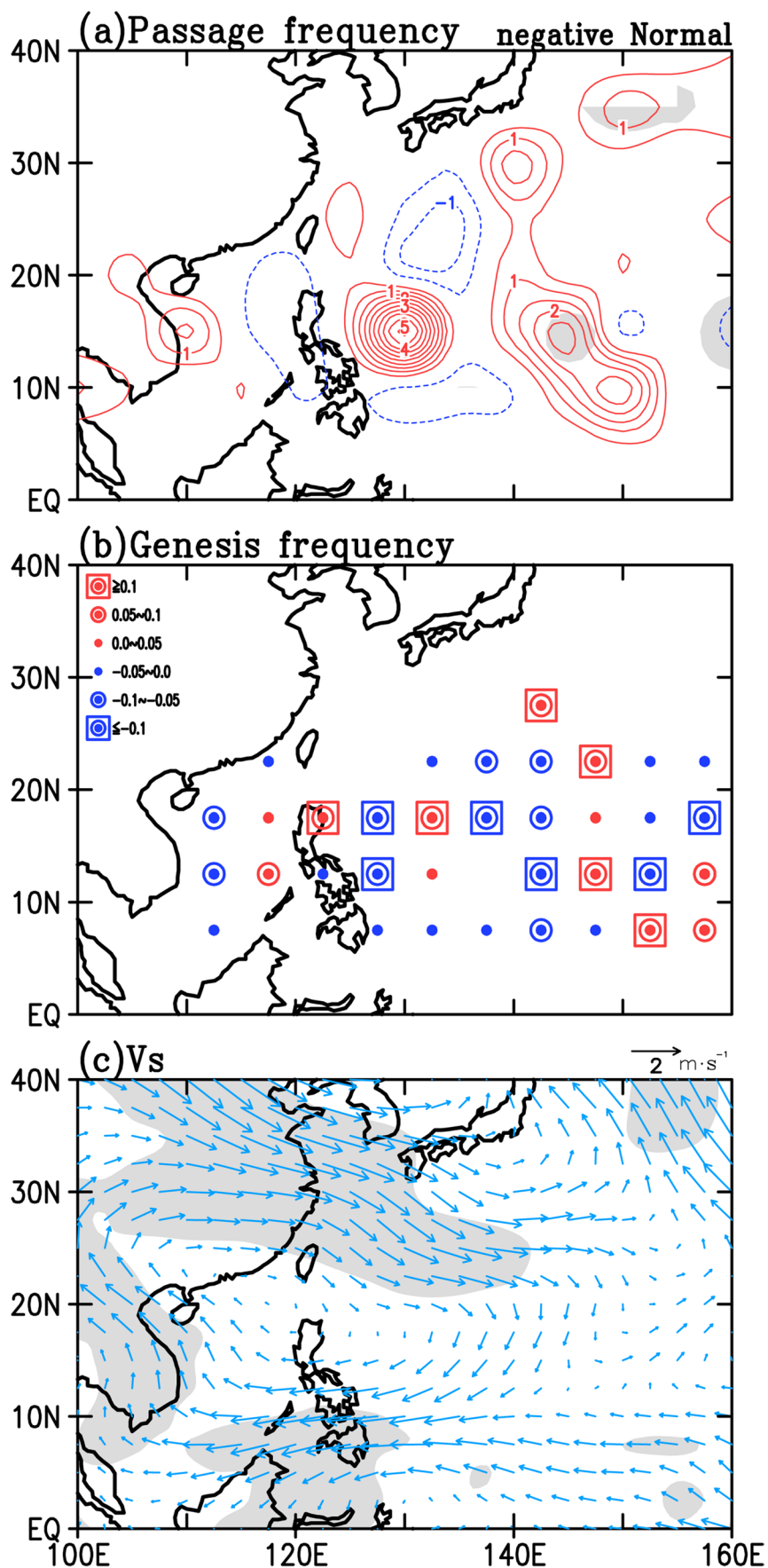
The NM+ and NM- types exhibit different modulating processes suppressing TC activity in Taiwan during October. In the NM+ type, cold SST anomalies in the tropical western WNP cause a divergent center in the 120°–130°E zone and an anomalous cyclone to the east of Taiwan. This anomalous cyclone guides TCs northward before reaching Taiwan. In the NM- type, warm SST anomalies extending from the western WNP westward into the eastern IO cause a westward-extended anomalous anticyclone across Taiwan

and the SCS. This anomalous anticyclone suppresses TC formation in the tropical western WNP and consequent movement toward Taiwan. These modulating processes result in zero October TCs in Taiwan in the NM+ and NM- types.

6 Concluding Remarks

TC activity affecting Taiwan reaches its peak phase in the July–September season and weakens evidently in October. During October, the chance for a TC forming in the WNP and later moving toward and affecting Taiwan was on average 0.36 during a 50-year period from 1970 to 2019. In this period, there were 32 years with no TCs affecting Taiwan, with only one TC per year for the other 18 years. The

Fig. 11 Same as in Fig. 3, except for the negative Normal (NM-) years



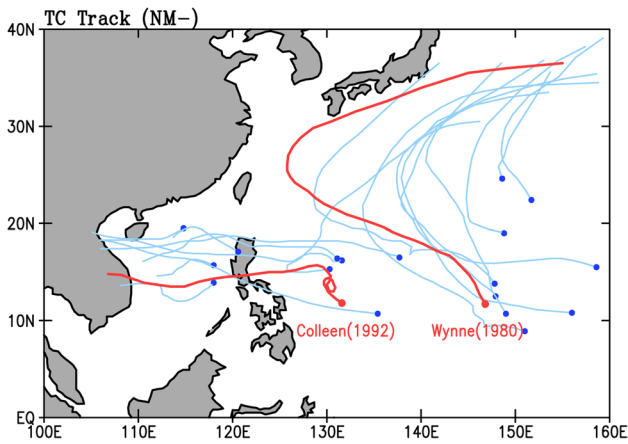
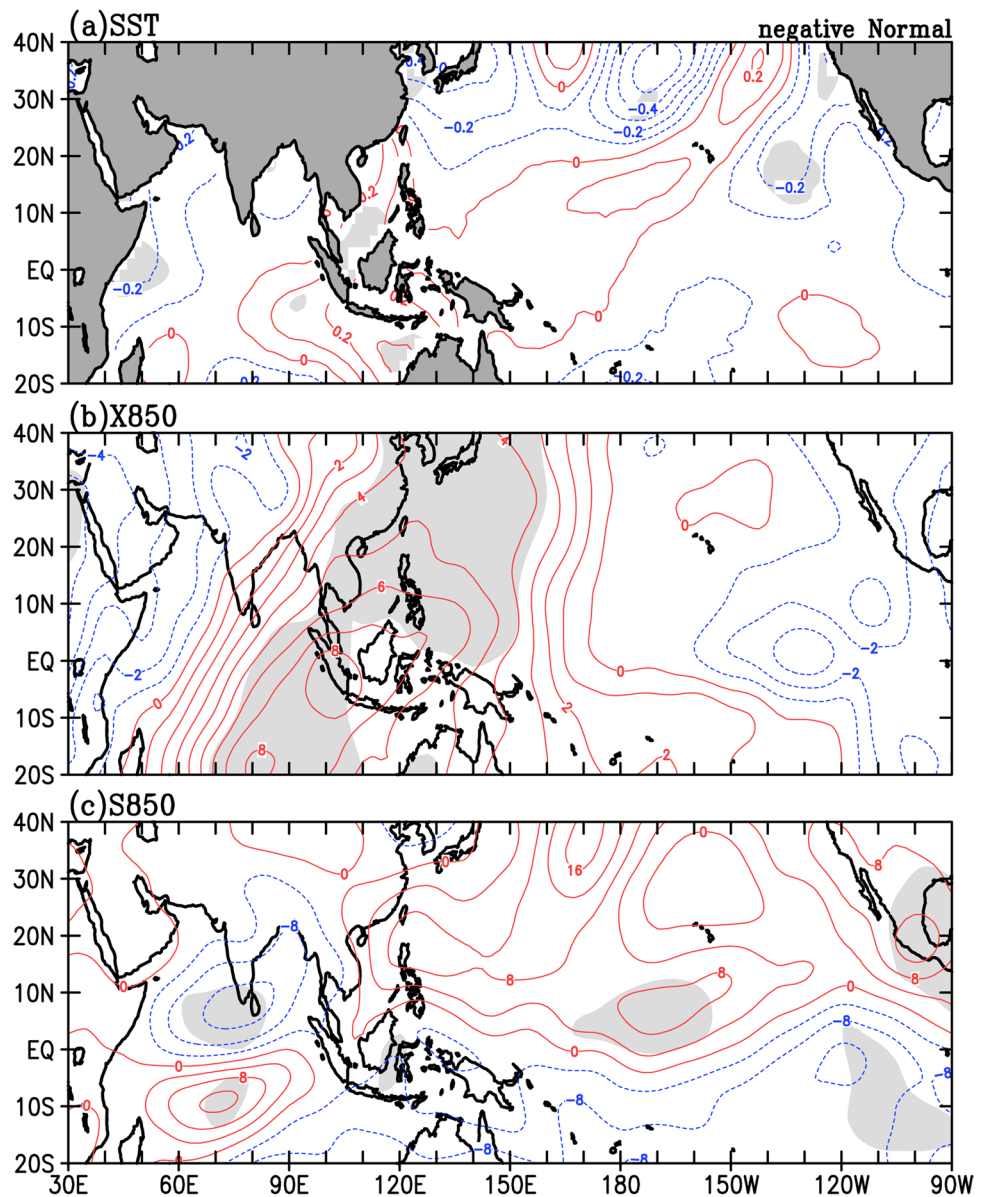


Fig. 12 Tracks of the October WNP TCs for the negative normal (NM-) years

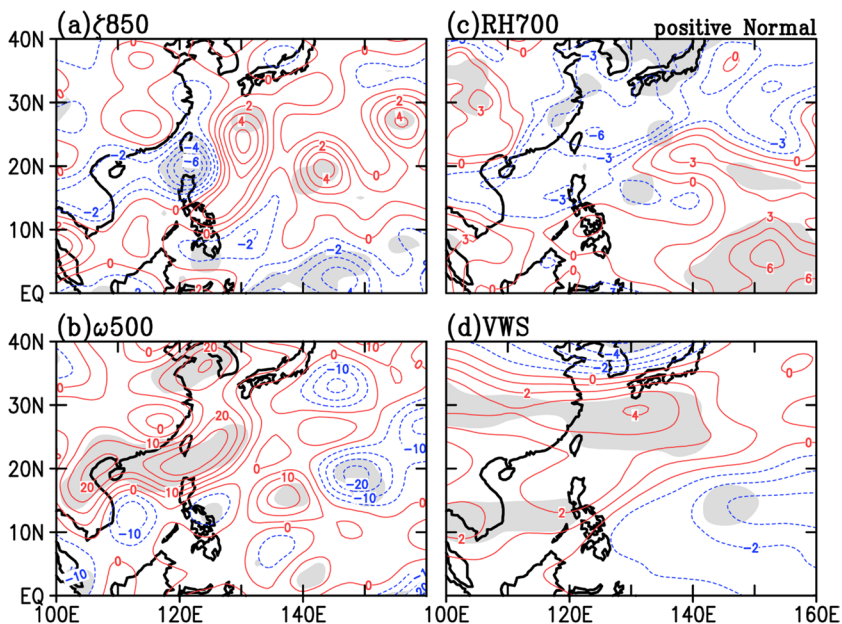
Fig. 13 Same as in Fig. 4, except for the negative Normal (NM-) years



dominance of zero TCs around Taiwan reflects the major suppressing effects of climatic factors. The main purpose of this study is to examine the suppressing effects exerted by different climatic factors on TC activity affecting Taiwan during October. Indexed by the September–November (SON) ONI value, the climatic conditions are separated into four types based on ENSO and non-ENSO (Normal) years: El Niño ($\geq 0.5\text{ }^{\circ}\text{C}$), La Niña ($\leq -0.5\text{ }^{\circ}\text{C}$), positive Normal ($0\text{--}0.5\text{ }^{\circ}\text{C}$), and negative Normal ($-0.5\text{--}0\text{ }^{\circ}\text{C}$). The modulating processes of these four climatic types to cause zero October TCs in Taiwan are illustrated via schematic diagrams in Fig. 16.

During Octobers of the El Niño type (Fig. 16a), the east–west contrast of tropical SST anomalies induces a large-scale anomalous divergent center (denoted by “DIV”) around the Maritime Continent. Via a Matsuno-Gill-type

Fig. 14 Same as in Fig. 7, except for positive Normal (NM+) years



response, the lower-level circulations respond with an anomalous anticyclone (denoted by “AC”) to the northwest of this divergent center and an anomalous cyclone (denoted by “C”) to the northeast. TC formation decreases in the western WNP to the southeast of Taiwan (denoted by “TC-”) due to significant reductions in upward motion and relative humidity. The northwestward TC movement is further hindered by anomalous westerly flows in the northern section of an anomalous anticyclonic circulation overlying the SCS,

leading to suppressed TC activity around Taiwan (denoted by a dashed blue arrow). On the other hand, increased TC formation in the eastern WNP is associated with significantly increased relative vorticity and weakened VWS. These TCs tend to move northwestward toward the anomalous cyclone over the WNP (denoted by a solid red arrow). As shown in Fig. 16b, the large-scale modulating processes in the La Niña type are largely in an opposite polarity to those of the El Niño type. A large-scale anomalous convergent center

Fig. 15 Same as in Fig. 7, except for negative Normal (NM-) years

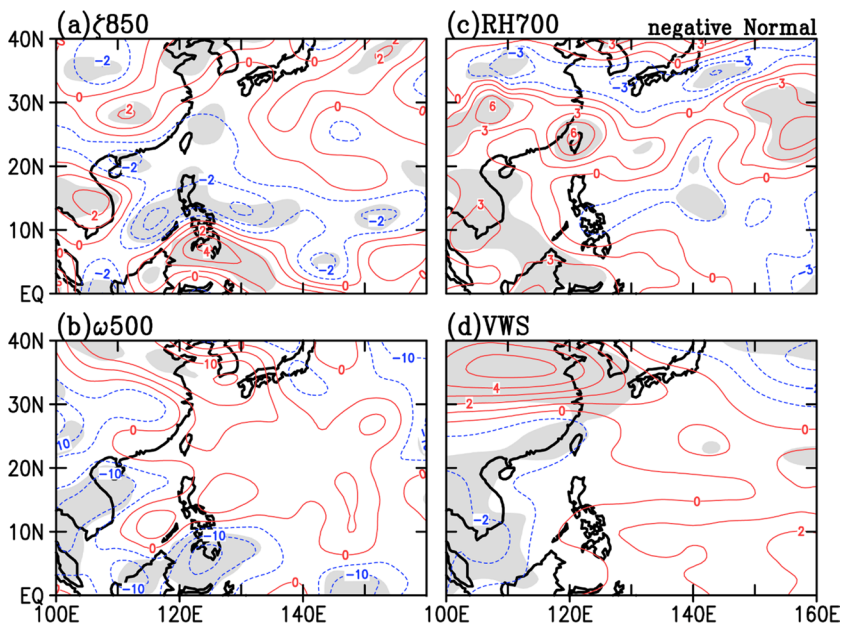


Table 3 Same as in Table 2, except for composite areal means of environmental factors affecting TC genesis in the non-ENSO types

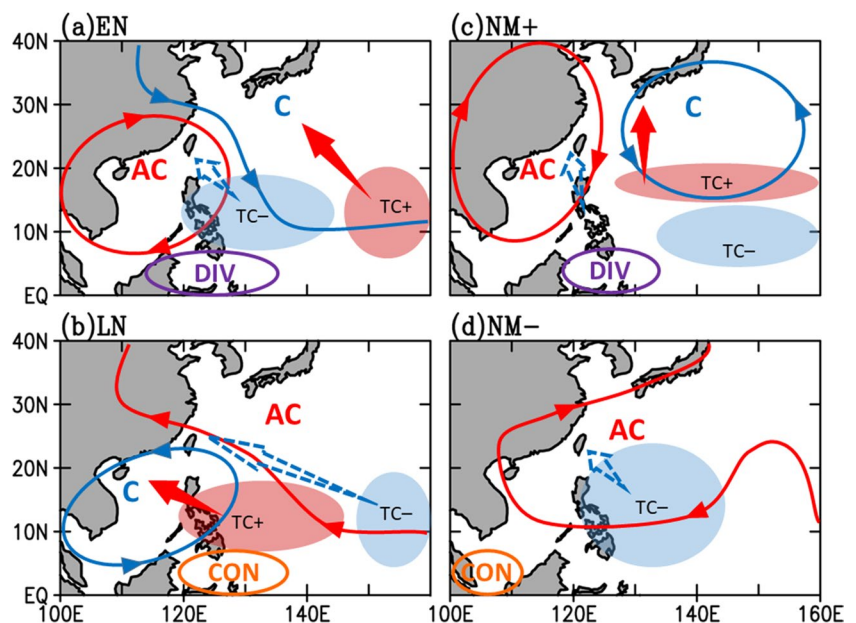
Climate type	Region	TC genesis	ζ_{850} (10^{-6} s^{-1})	ω_{500} ($10^{-3} \text{ Pa s}^{-1}$)	RH700 (%)	VWS (m s^{-1})
NM+	130° -160°E 5° -15°N	decreased	-0.40	2.26	2.12*	-2.09
	125° -160°E 15° -20°N	increased	1.24*	-1.35	1.03*	-0.86
NM-	120° -145°E 5° -25°N	decreased	-0.52	-0.60	0.0	0.33

(denoted by “CON”) occurs around the Maritime Continent. It is accompanied with an anomalous cyclone to the northwest across the SCS and an anomalous anticyclone to the northeast over the WNP. TC formation increases in the western WNP due to significant increases of upward motion and relative humidity. These TCs are guided by anomalous southeasterly flows of an anomalous cyclone toward the SCS. TC formation in the eastern WNP decreases in association with reduced relative vorticity and enhanced VWS and results in reduced TC movement toward Taiwan. These processes jointly result in suppressed TC activity around Taiwan. TC genesis in the ENSO types is systematically modulated by significant variability of vertical motion and relative humidity in the western WNP, but by significant changes of relative vorticity and VWS in the eastern WNP.

For the non-ENSO types, Octobers of the positive Normal type feature positive SST anomalies in the tropical Pacific east of 150°E and negative SST anomalies to the west. As shown in Fig. 16c, this SST contrast induces a large-scale anomalous divergent center near the Maritime Continent.

An anomalous anticyclone appears on the northwestern side of the anomalous divergent center across the SCS and eastern China, while an anomalous cyclone on the northeastern side elongates in the subtropical WNP. TC genesis tends to increase in the southern sector of the anomalous cyclone over the 15°-20°N zone of the WNP assisted by significantly enhanced relative vorticity and relative humidity. TC genesis decreases in the more southern regions over the 5°-15°N zone mainly caused by reductions in relative vorticity and upward motion. Increased TCs are guided by the anomalous cyclonic flows northward toward its central region. The anomalous anticyclone across the SCS and Taiwan exerts anomalous northwesterly flows to block TC movement toward Taiwan. These processes together suppress TC activity around Taiwan. For the negative Normal type (Fig. 16d), the salient features are warm SST anomalies extending westward from the tropical WNP into the eastern Indian Ocean, leading to a westward-shifted anomalous convergent center in the 100°-110°E region. Consequently, the anomalous anticyclone to the northeast of this convergent

Fig. 16 The schematic diagrams illustrate the major modulating processes suppressing TC activity around Taiwan by the (a) EN, (b) LN, (c) NM+, and (d) NM- types. The anomalous cyclonic/anticyclonic circulation is denoted by “C”/“AC”. The increased/decreased TC genesis is portrayed by red/blue shading and denoted by “TC+”/“TC-”. The increased/decreased passage frequency is denoted by a solid red/dashed blue arrow. The anomalous lower-level convergent/divergent center is denoted by “CON”/“DIV”



center also extends westward from the WNP across Taiwan into the SCS. This anomalous anticyclone weakens TC genesis over its southern sector via reduced relative vorticity and enhanced VWS. The anomalous anticyclonic circulation overlying Taiwan acts to steer TCs from the WNP toward the SCS, leading to suppressed TC activity around Taiwan. Relative vorticity is the only factor to positively affect TC genesis variability in both the positive and negative Normal types, reflecting the important role of overlying circulation anomalies in modulating TC activity under the non-ENSO conditions.

Either zero TCs or one TC affects Taiwan in October for the period 1970–2019. TCs in the one-TC years approach Taiwan via different track types across every sectors of the impact region surrounding Taiwan (not shown), implicating the possible existence of different large-scale steering flows within each climate type. On the other hand, the zero-TC cases have no TCs in the region surrounding Taiwan, which reflects a common feature in TC activity among these cases. This common feature should to some extent reduce the randomness in the results of zero-TC analyses. Moreover, zero-TC cases are shown to be systematically modulated by large-scale anomalies of SST, X850, S850, and steering flows that move TCs away from Taiwan. These anomalies are significant in both the ENSO and non-ENSO types due to their large-scale features. However, genesis frequency and passage frequency are generally less significant in their composite anomalies due to the chaotic spatial distribution of TC activity. The large-scale anomalies exhibit clear dynamic processes to explain the suppression of TC activity around Taiwan for different climatic conditions, even though TC-related anomalies are not particularly significant. These large-scale processes can serve as useful guidance for projecting TC variability over the WNP and Taiwan.

The major circulation features suppressing October TC activity around Taiwan exhibit distinct patterns among these four climatic types. TCs mainly move northwestward toward Taiwan from the tropical WNP to the southeast of Taiwan. In this region, TC genesis decreases in both the El Niño and negative Normal types, but increases in the La Niña and positive Normal types. The decreased TCs are further blocked for northwestward movement by an anomalous anticyclone over the SCS in the El Niño type, but by a westward-extended anomalous anticyclone across the WNP and SCS in the negative Normal types. On the other hand, increased TCs are guided by an anomalous cyclone toward the SCS to the southwest of Taiwan in the La Niña type, but toward the subtropical WNP to the east of Taiwan in the positive Normal type. Suppression of TC activity in Taiwan during October appears to result from combined changes in TC genesis locations and steering flows associated with large-scale circulation anomalies. These circulation features in different climatic types can serve as monitoring targets for seasonal

predictions of October TC activity over Taiwan and the surrounding regions.

Acknowledgements We would like to thank anonymous reviewers for their valuable comments to improve this paper. This study was supported by the Ministry of Science and Technology, Taiwan, under grants MOST 111-2611-M-110-013 and MOST 111-2111-M-992-001.

Data Availability All datasets analyzed in this study can be freely downloaded from the open websites. The NCEP-NCAR reanalysis data are available from the Physical Sciences Laboratory, NOAA, at <https://psl.noaa.gov/data/gridded/data.ncep.reanalysis.pressure.html>. The monthly ERSST-5 data are available at <https://www1.ncdc.noaa.gov/pub/data/cmb/ersst/v5/netcdf/>. The ONI data are available from the Climate Prediction Center, NOAA, at <https://www.cpc.ncep.noaa.gov/products/precip/CWlink/MJO/enso.shtml#history>. The best-track data are available from JTWC at <https://www.metoc.navy.mil/jtwc/jtwc.html?western-pacific>.

References

- Camargo, S.J., Robertson, A.W., Gaffney, S.J., Smyth, P., Ghil, M.: Cluster analysis of typhoon tracks: Part I: General properties. *J. Clim.* **20**(14), 3635–3653 (2007). <https://doi.org/10.1175/JCLI4188.1>
- Camargo, S.J., Sobel, A.H.: Western North Pacific tropical cyclone intensity and ENSO. *J. Clim.* **18**(15), 2996–3006 (2005). <https://doi.org/10.1175/JCLI3457.1>
- Chan, J.C.L.: Tropical cyclone activity over the western North Pacific associated with El Niño and La Niña events. *J. Clim.* **13**(16), 2960–2972 (2000). [https://doi.org/10.1175/1520-0442\(2000\)013%3c2960:TCAOTW%3e2.0.CO;2](https://doi.org/10.1175/1520-0442(2000)013%3c2960:TCAOTW%3e2.0.CO;2)
- Chen, C.-S., Chen, Y.-L., Liu, C.-L., Lin, P.-L., Chen, W.-C.: Statistics of heavy rainfall occurrences in Taiwan. *Weather Forecast.* **22**(5), 981–1002 (2007). <https://doi.org/10.1175/WAF1033.1>
- Chen, C.-S., Chen, Y.-L.: The rainfall characteristics of Taiwan. *Mon. Weather Rev.* **131**(7), 1323–1341 (2003). [https://doi.org/10.1175/1520-0493\(2003\)131%3c1323:TRCOT%3e2.0.CO;2](https://doi.org/10.1175/1520-0493(2003)131%3c1323:TRCOT%3e2.0.CO;2)
- Chen, J.-M., Chen, H.-S., Liu, J.-S.: Coherent interdecadal variability of tropical cyclone rainfall and seasonal rainfall in Taiwan during October. *J. Clim.* **26**(1), 308–321 (2013a). <https://doi.org/10.1175/JCLI-D-11-00697.1>
- Chen, J.-M., Chen, H.-S.: Interdecadal variability of summer rainfall in Taiwan associated with tropical cyclones and monsoon. *J. Clim.* **24**(22), 5786–5798 (2011). <https://doi.org/10.1175/2011JCLI4043.1>
- Chen, J.-M., Li, T., Shih, C.-F.: Tropical cyclone and monsoon induced rainfall variability in Taiwan. *J. Clim.* **23**(15), 4107–4120 (2010). <https://doi.org/10.1175/2010JCLI3355.1>
- Chen, J.-M., Lin, P.-H., Wu, C.-H., Sui, C.-H.: Track variability of South China Sea-formed tropical cyclones modulated by seasonal and intraseasonal circulations. *Terr. Atmos. Ocean. Sci.* **31**(2), 239–259 (2020). <https://doi.org/10.3319/TAO.2019.11.07.02>
- Chen, J.-M., Tan, P.-H., Shih, C.-F.: Heavy rainfall induced by tropical cyclones across northern Taiwan and associated intraseasonal oscillation modulation. *J. Clim.* **26**(20), 7992–8007 (2013b). <https://doi.org/10.1175/JCLI-D-12-00692.1>
- Chen, J.-M., Tan, P.-H., Wu, L., Chen, H.-S., Liu, J.-S., Shih, C.-F.: Interannual variability of summer tropical cyclone rainfall in the western North Pacific depicted by CFSR and associated large-scale processes and ISO modulations. *J. Clim.* **31**(5), 1771–1787 (2018a). <https://doi.org/10.1175/JCLI-D-16-0805.1>



- Chen, J.-M., Tan, P.-H., Wu, L., Liu, J.-S., Chen, H.-S.: Climatological analysis of passage-type tropical cyclones from the Western North Pacific into the South China Sea. *Terr. Atmos. Ocean. Sci.* **28**(3), 327–343 (2017). <https://doi.org/10.3319/TAO.2016.10.04.02>
- Chen, J.-M., Wu, C.-H., Chung, P.-H., Sui, C.-H.: Influence of intra-seasonal-interannual oscillations on tropical cyclone genesis in the Western North Pacific. *J. Clim.* **31**(12), 4949–4961 (2018b). <https://doi.org/10.1175/JCLI-D-17-0601.1>
- Chen, J.-M., Wu, C.-H., Gao, J., Chung, P.-H., Sui, C.-H.: Migratory tropical cyclones in the South China Sea modulated by intraseasonal oscillations and climatological circulations. *J. Clim.* **32**(19), 6445–6466 (2019). <https://doi.org/10.1175/JCLI-D-18-0824.1>
- Chen, T.-C., Wang, S.-Y., Yen, M.-C., Clark, A.J.: Impact of the intraseasonal variability of the western North Pacific large-scale circulation on tropical cyclone tracks. *Weather Forecast.* **24**(3), 646–666 (2009). <https://doi.org/10.1175/2008WAF2222186.1>
- Chen, T.-C., Wang, S.-Y., Yen, M.-C.: Interannual variation of the tropical cyclone activity over the western North Pacific. *J. Clim.* **19**(21), 5709–5720 (2006). <https://doi.org/10.1175/JCLI3934.1>
- Chia, H.-H., Ropelewski, C.F.: The interannual variability in the genesis location of tropical cyclones in the northwest Pacific. *J. Clim.* **15**(20), 2934–2944 (2002). [https://doi.org/10.1175/1520-0442\(2002\)015%3c2934:TIVITG%3e2.0.CO;2](https://doi.org/10.1175/1520-0442(2002)015%3c2934:TIVITG%3e2.0.CO;2)
- Chu, P.-S., Murakami, H.: *Climate variability and tropical cyclone activity*, Cambridge University Press, New York, 320 pp (2022)
- Chu, P.-S., Zhao, X., Kim, C.-H., Kim, H.-S., Lu, M.-M., Kim, J.-H.: Bayesian forecasting of seasonal typhoon activity: A track-pattern-oriented categorization approach for Taiwan. *J. Clim.* **23**(24), 6654–6668 (2010). <https://doi.org/10.1175/2010JCLI3710.1>
- Gill, A.E.: Some simple solutions for heat-induced tropical circulation. *Quart. J. Royal Meteor. Soc.* **106**(449), 447–462 (1980). <https://doi.org/10.1002/qj.49710644905>
- Gray, W.M.: Global view of the origin of tropical disturbances and storms. *Mon. Weather Rev.* **96**(10), 669–700 (1968). [https://doi.org/10.1175/1520-0493\(1968\)096%3c0669:GVOTOO%3e2.0.CO;2](https://doi.org/10.1175/1520-0493(1968)096%3c0669:GVOTOO%3e2.0.CO;2)
- Ha, Y., Zhong, Z., Yang, X., Sun, Y.: Contribution of East Indian Ocean SSTA to western North Pacific tropical cyclone activity under El Niño/La Niña conditions. *Int. J. Climatol.* **35**(4), 506–519 (2015). <https://doi.org/10.1002/joc.3997>
- Harr, P.A., Elsberry, R.L.: Tropical cyclone track characteristics as a function of large-scale circulation anomalies. *Mon. Weather Rev.* **119**(6), 1448–1468 (1991). [https://doi.org/10.1175/1520-0493\(1991\)119%3c1448:TCTCAA%3e2.0.CO;2](https://doi.org/10.1175/1520-0493(1991)119%3c1448:TCTCAA%3e2.0.CO;2)
- Holliday, C.R., Thompson, A.H.: Climatological characteristics of rapidly intensifying typhoons. *Mon. Weather Rev.* **107**(8), 1022–1034 (1979). [https://doi.org/10.1175/1520-0493\(1979\)107%3c1022:CCORIT%3e2.0.CO;2](https://doi.org/10.1175/1520-0493(1979)107%3c1022:CCORIT%3e2.0.CO;2)
- Hsu, P.-C., Chu, P.-S., Murakami, H., Zhao, X.: An abrupt decrease in the late-season typhoon activity over the western North Pacific. *J. Climate* **27**(11), 4296–4312 (2014). <https://doi.org/10.1175/JCLI-D-13-00417.1>
- Huang, B., Throne, P.W., Banzon, V.F., Boyer, T., Chepurin, G., Lawrimore, J.H., Menne, M.J., Smith, T.M., Vose, R.S., Zhang, H.-M.: Extended Reconstructed Sea Surface Temperature version 5 (ERSSTv5), Upgrades, validations, and intercomparisons. *J. Clim.* **30**(20), 8179–8205 (2017a). <https://doi.org/10.1175/JCLI-D-16-0836.1>
- Huang, H.-C., Boucharel, J., Lin, I.-I., Jin, F.-F., Lien, C.-C., Pan, I.-F.: Air-sea fluxes for hurricane Patricia (2015): comparison with supertyphoon Haiyan (2013) and under different ENSO conditions. *J. Geophys. Res. Oceans* **122**(8), 6067–6089 (2017b). <https://doi.org/10.1002/2017JC012741>
- Kalnay, E., et al.: The NCEP/NCAR 40-year reanalysis project. *Bull. Am. Meteorol. Soc.* **77**(3), 437–471 (1996). [https://doi.org/10.1175/1520-0477\(1996\)077<0437:TNYRP>2.0.CO;2](https://doi.org/10.1175/1520-0477(1996)077<0437:TNYRP>2.0.CO;2)
- Kaplan, J., DeMaria, M.: Large-scale characteristics of rapidly intensifying tropical cyclones in the North Atlantic basin. *Weather Forecast.* **18**(6), 1093–1108 (2003). [https://doi.org/10.1175/1520-0434\(2003\)018%3c1093:LCORIT%3e2.0.CO;2](https://doi.org/10.1175/1520-0434(2003)018%3c1093:LCORIT%3e2.0.CO;2)
- Lai, T.-L., Chen, J.-M., Sui, C.-H., Tan, P.-H., Wu, L., Tsai, M.-Y.: Interannual variability of summer tropical cyclone activity in the northwestern North Pacific modulated by El Niño–Southern Oscillation and intraseasonal oscillation. *Int. J. Climatol.* **41**(14), 6283–6299 (2021). <https://doi.org/10.1002/joc.7194>
- Lai, T.-L., Chen, J.-M., Tan, P.-H., Tu, J.-Y., Chen, H.-S., Chen, C.-H.: Modulations of El Niño–Southern Oscillation on tropical cyclone activity affecting Taiwan. *Atmos. Res.* **279**, 106366 (2022). <https://doi.org/10.1016/j.atmosres.2022.106366>
- Lander, M.A.: Specific tropical cyclone track types and unusual tropical cyclone motions associated with a reverse-oriented monsoon trough in the western North Pacific. *Weather Forecast.* **11**(2), 170–186 (1996). [https://doi.org/10.1175/1520-0434\(1996\)011%3c0170:STCTTA%3e2.0.CO;2](https://doi.org/10.1175/1520-0434(1996)011%3c0170:STCTTA%3e2.0.CO;2)
- Li, R.C.Y., Zhou, W.: Modulation of western North Pacific tropical cyclone activity by the ISO. Part II: Tracks and landfall. *J. Clim.* **26**(9), 2919–2930 (2013). <https://doi.org/10.1175/JCLI-D-12-00211.1>
- Li, W.-T., Chen, J.-M., Tseng, R.-S., Lai, T.-L.: Multiple modulating processes for intensive tropical cyclone activity affecting Taiwan in September 2016. *Asia-Pacific J. Atmos. Sci.* **58**(1), 145–157 (2022). <https://doi.org/10.1007/s13143-021-00245-2>
- Matsuno, T.: Quasi-geostrophic motions in the equatorial area. *J. Meteorol. Soc. Jpn.* **44**(1), 25–43 (1966). https://doi.org/10.2151/jmsj1965.44.1_25
- McPhaden, J.J.: Genesis and evolution of the 1997–1998 El Niño. *Science* **283**(5404), 950–954 (1999). <https://doi.org/10.1126/science.283.5404.950>
- Shan, K., Yu, X.: Interdecadal variability of tropical cyclone genesis frequency in western North Pacific and South Pacific Ocean basins. *Environ. Res. Lett.*, 15(6), 064030 (2020a). <https://doi.org/10.1088/1748-9326/ab8093>
- Shan, K., Yu, X.: A simple trajectory model for climatological studies of tropical cyclones. *J. Climate* **33**(18), 7777–7786 (2020b). <https://doi.org/10.1175/JCLI-D-20-0285.1>
- Shan, K., Yu, X.: Variability of tropical cyclone landfalls in China. *J. Climate* **34**(23), 9235–9247 (2021). <https://doi.org/10.1175/JCLI-D-21-0031.1>
- Tan, P.-H., Tu, J.-Y., Wu, L., Chen, H.-S., Chen, J.-M.: Asymmetric relationships between ENSO and entrance tropical cyclones in the South China Sea during fall. *Int. J. Climatol.* **39**(4), 1872–1888 (2019). <https://doi.org/10.1002/joc.5921>
- Tippett, M.K., Camargo, S.J., Sobel, A.H.: A Poisson regression index for tropical cyclone genesis and the role of large-scale vorticity in genesis. *J. Clim.* **24**(9), 2335–2357 (2011). <https://doi.org/10.1175/2010JCLI3811.1>
- Tu, J.-Y., Chen, J.-M., Tan, P.-H., Lai, T.-L.: Seasonal contrasts between tropical cyclone genesis in the South China Sea and westernmost North Pacific. *Int. J. Climatol.* **42**(7), 3743–3756 (2022). <https://doi.org/10.1002/joc.7442>
- Wu, L., Zhang, H.-J., Chen, J.-M., Feng, T.: Impact of two types of El Niño on tropical cyclones over the western North Pacific: sensitivity to location and intensity of Pacific warming. *J. Clim.* **31**(5), 1725–1742 (2018). <https://doi.org/10.1175/JCLI-D-17-0298.1>
- Wu, R., Yang, Y.-Y., Cao, X.: Respective and combined impacts of regional SST anomalies on tropical cyclogenesis in different sectors of the western North Pacific. *J. Geophys. Res.-Atmos.*

- 124**(16), 8917–8934 (2019). <https://doi.org/10.1029/2019JD030736>
- Xue, Y., Smith, T.M., Reynolds, R.W.: Interdecadal changes of 30-yr SST normals during 1871–2000. *J. Clim.* **16**(10), 1601–1612 (2003). [https://doi.org/10.1175/1520-0442\(2003\)016%3c1601:ICOYSN%3e2.0.CO;2](https://doi.org/10.1175/1520-0442(2003)016%3c1601:ICOYSN%3e2.0.CO;2)
- Yeh, S.-W., Kug, J.-S., Dewitte, B., Kwon, M.-H., Kirtman, B.P., Jin, F.-F.: El Niño in a changing climate. *Nature* **461**, 511–514 (2009). <https://doi.org/10.1038/nature08316>
- Yu, J., Li, T., Tan, Z., Zhu, Z.: Effects of tropical North Atlantic SST on tropical cyclone genesis in the western North Pacific. *Clim. Dyn.* **46**(3–4), 865–877 (2016). <https://doi.org/10.1007/s00382-015-2618-x>
- Zhan, R., Wang, Y., Lei, X.: Contributions of ENSO and East Indian Ocean SSTA to the interannual variability of northwest Pacific tropical cyclone frequency. *J. Clim.* **24**(2), 509–521 (2011). <https://doi.org/10.1175/2010JCLI3808.1>

Publisher's Note Springer Nature remains neutral with regard to jurisdictional claims in published maps and institutional affiliations.

Springer Nature or its licensor (e.g. a society or other partner) holds exclusive rights to this article under a publishing agreement with the author(s) or other rightsholder(s); author self-archiving of the accepted manuscript version of this article is solely governed by the terms of such publishing agreement and applicable law.